Available online at www.sciencedirect.com
ScienceDirect
Journal of Nuclear Materials 363–365 (2007) 242–246
journal of nuclear materials
www.elsevier.com/locate/jnucmat

Discharge resolved impurity flux measurements in the edge plasma of ASDEX Upgrade by exposure of collector probes

W. Schustereder *, K. Krieger [1], A. Herrmann, V. Rohde, ASDEX Upgrade Team

Max-Planck-Institut für Plasmaphysik, EURATOM Assoziation, Boltzmannstraße 2, D-85748 Garching, Germany

Abstract

The exposure of collector probes using the ASDEX Upgrade midplane manipulator allowed to quantify the particle fluxes at the outer midplane. Time resolved measurements were carried out employing rotating cylindrical samples shielded by a narrow slit aperture. After exposure the retrieved probes were analyzed ex-situ using Rutherford back-scattering (RBS), nuclear reaction analysis (NRA) and proton induced X-ray emission (PIXE). Time resolved measurements allow to correlate impurity fluxes with well defined discharge conditions. Increased deposition is observed within the low density start-up phase as well as in configurations with small separatrix-sample distance and increased ICRH heating. Quantification of implanted deuterium as well as W and other impurity species was carried out and compared to spectroscopic data. Radial scans revealed an exponential fall-off of all species with radial decay lengths varying between ~2.5 mm (Fe) and ~6–10 mm (D). Also the origin of prominent impurities like Ca is clarified.

PACS: 28.52.Fa; 52.25.Vy; 52.40.Hf

Keywords: ASDEX Upgrade; Erosion and deposition; Impurity; Probes; Tungsten

1. Introduction

Erosion and deposition are crucial issues in fusion research because of their impact on plasma contamination, the lifetime of plasma-facing components and tritium inventories. Tungsten is considered as material choice for plasma-facing components in ITER [1] due to its high sputtering threshold energy, low sputtering yield and small tritium retention. It has been successfully employed in ASDEX Upgrade with increasing percentage of coverage over the last years which will ultimately lead to a full tungsten machine in 2007 [2]. However, tungsten is a high Z material, which can substantially contribute to radiation cooling. ITER will only allow a concentration of $c_w = 2 \times 10^{-5}$ [3].

In recent years test tiles were exposed in various machines as plasma facing components. After a full experimental campaign they were retrieved and analysed with ion beam methods [4,5]. This approach allows, however, only to determine integrated

* Corresponding author. Fax: +49 89 3299 1212.
E-mail addresses: Werner.Schustereder@ipp.mpg.de (W. Schustereder), Karl.Krieger@ipp.mpg.de (K. Krieger).
[1] Presenting author.

0022-3115/$ - see front matter
doi:10.1016/j.jnucmat.2007.01.011

erosion and deposition fluxes over different discharge scenarios. To get a hold on the particle fluxes at the outer midplane for well defined discharge conditions, discharge resolved measurements and even time resolved measurements within one discharge were performed by exposure of collector samples using the ASDEX Upgrade midplane manipulator.

2. Experimental

The exposed samples are cylinders made of highly pure graphite with a length of 88 mm and a diameter of 30 mm. They are exposed to discharges using the midplane manipulator system of ASDEX Upgrade (Fig. 1), located at $z = 0.31$ m above the midplane in the shadow of an ICRH limiter and near a protection limiter. To obtain a well defined plasma wetted surface, the samples were mounted inside a graphite shield with a narrow slit aperture defining a viewing cone of 12°. The slit is oriented parallel to the sample in radial direction (Fig. 1). Exposure was mainly done in stationary H-mode discharges in lower single null configuration with a current of $I_P = 0.8$–1 MA, a toroidal field of $B_t = -2.5$ T and line averaged densities between $n_e = 5$–7×10^{19} m^{-3}. Apart from time integrated discharge exposures using fixed samples time resolved measurements were also carried out employing rotating cylindrical samples with a rotation speed of 10° s^{-1}, resulting in a time resolution of ~1.2 s. After exposure the retrieved probes were analyzed ex-situ using Rutherford back-scattering (RBS), nuclear reaction analysis (NRA) and proton induced X-ray emission (PIXE).

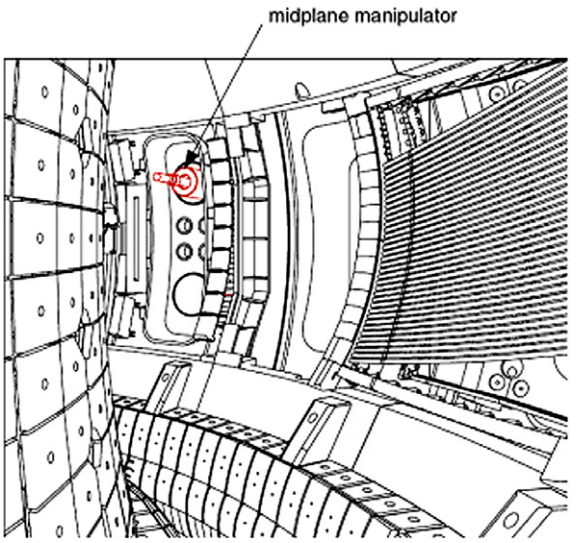

Fig. 1. Position of the ASDEX midplane manipulator system at $z = 0.31$ m above the equatorial midplane.

Rutherford back-scattering (RBS) spectra were taken employing $^3He^+$ ions at 0.8 MeV as well as $^7Li^+$ ions at 1 MeV with perpendicular impact of the projectiles on the samples. Recoil ions were detected at a scattering angle of 165°. An ion charge of 10 μC in the case of $^3He^+$ and 20 μC for $^7Li^+$, respectively, was typically acquired for each spectrum. The resolution for heavy elements like Fe and W is good, allowing accurate quantification of areal densities of these plasma impurities on the sample. SIMNRA 5.84 [6] was used as source of cross section data and as a tool for simulation and fitting of the RBS spectra. Signals of mid- and low-Z materials are often overlapping with those of other elements, making quantitative statements difficult.

Therefore the amount of mid- and low-Z trace elements deposited onto the samples was additionally quantified by particle-induced X-ray emission (PIXE) using a 1.5 MeV proton beam. The detection of characteristic X-ray lines from all elements heavier than F allowed quantitative analysis using cross section data published by Paul and Sacher [7]. Due to the sharp line width signals are usually nearly free from interference with characteristic lines from other chemical elements. Compared with RBS, this technique has in general a lower sensitivity but a higher resolution.

The near-surface amounts of deuterium were measured by nuclear reaction analysis (NRA) using the reaction $^3He(d,p)\alpha$. The analyzing depth with the employed incident $^3He^+$ energy of 800 keV is in the range of 1 μm. Quantification is achieved by comparison to reference samples with a-C:D layers of known thickness and composition.

3. Results

3.1. Discharge resolved measurements

Discharge integrated exposures show a clear correlation of impurity amount collected at the probe with applied ICRH power in combination with the distance d_{SP} of the separatrix to the probe. Already by observing the increase of W deposited at the probe with decreasing d_{SP} the radial decay length (RDL) can be estimated, resulting in typical RDLs (W) in the limiter shadow of 4–6 mm. Apart from

ICRH power and d_{SP} also increased ELM activity enhances the flux of impurities onto the sample because of the ion temperature rising [8], resulting in W sputtering by hot deuterium.

3.2. Time resolved measurements

Time resolved measurements allow the quantification of the deuterium flux as well as the flux of W and other impurities at each phase of a discharge. As a typical example ASDEX Upgrade discharge #20823 is described in more detail, a stationary H-mode discharge in lower single null configuration with a current of $I_P = 0.8$ MA, a toroidal field of $B_t = -2.5$ T, line averaged density of $n_e = 5 \times 10^{19}$ m^{-3}, auxiliary heating power by neutral beams $P_{NBI} = 5$ MW and a long flat-top phase $t = 0.8$–8.3 s. Fig. 2 shows time traces of the D and W flux to the probe together with spectroscopic measurements of the D recycling flux and W erosion flux at an adjacent W-coated limiter. Especially during the start-up phase, the low density plasma is sufficiently hot for W sputtering (Fig. 2, $t = 1.5$ s). Furthermore, during the discharge a variation of the radial plasma position was carried out. During the R_{sep} scan the distance d between the separatrix and the collector probe was varied as follows: $d \approx 80$ mm from $t = 2$–4 s, $d \approx 70$ mm ($t = 4$–6 s) and $d \approx 60$ mm ($t = 6$–8 s). As a result of the outward shift both the deuterium and impurity fluxes (shown here for W) increase. Comparison of areal densities detected on the collector sample to time integrated ($\delta t = 1$ s) spectroscopic data taken from a line-of-sight that is directed at a position of $z = 0.28$ m on an ICRH limiter (Fig. 2) show a very good qualitative agreement, whereas the absolute value differs significantly. This can be explained by the fact that the areal densities are measured at a sample position of 16 mm behind the limiter edge. At this radius both, D and W, signals show a plateau instead of the expected exponential increase towards the limiter edge (Fig. 3). In the case of D this can be explained by the high probe temperature (≈200 °C at the sample tip). W, however, seems to be sputtered by the simultaneously incident iron flux. TRIDYN calculates the sputter yield of Fe on W to be ~1% at $E_{Fe} = 50$ eV which is a reasonable energy ($T_e \leqslant 20$ eV [9]). Taking into account the ratio of ~50:1 of Fe collected compared to W this explains the flattening of the W radial profile. This also fits perfectly to the observation that the amount of collected W is even decreasing towards the limiter edge because of the impact of Fe ions with higher energies, and a corresponding sputter yield of ~10% at $E_{Fe} = 100$ eV. Taking the exponential part of the radial scans one can calculate the limiter shadow RDL for different phases of a discharge. During the start-up at $t = 1$ s, RDL (Fe, Cr, Ni, W) ≈ 2–3 mm and RDL (D) ≈ 6 mm are measured. These values are smaller than the

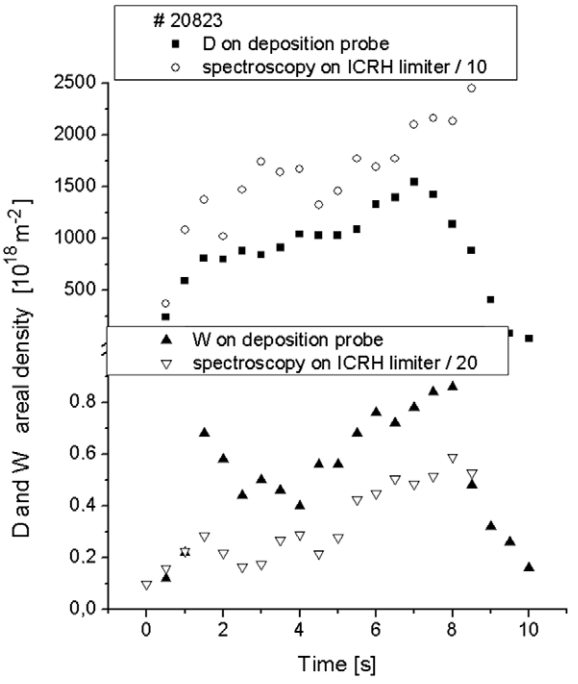

Fig. 2. ASDEX Upgrade discharge #20823 was used for R_{sep} scans. Time traces of D and W deposition on the pyrolytic graphite sample exposed by the midplane manipulator together with spectroscopic data of particle fluxes on a nearby position at the midplane are presented.

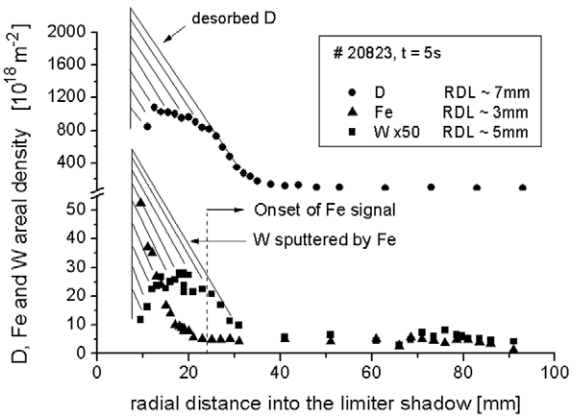

Fig. 3. Radial profiles of the measured areal density of D, W and Fe for the flat-top phase of #20823. The dashed areas illustrate the desorbed D and the W sputtered by Fe, respectively.

ones found during the flat-top phase (measured at $t = 5$ s) with RDL (Fe) ≈ 3 mm, RDL (Cr, Ni, W) ≈ 5 mm and RDL (D) ≈ 7 mm as well as during ramp-down at $t = 8.5$ s with RDL (Fe) ≈ 5 mm, RDL (Cr, Ni, W) ≈ 6 mm and RDL (D) ≈ 10 mm. From the increase of the measured W flux due to the R_{sep} scan a RDL for the scrape-off layer of $\approx$25 mm (spectroscopic data) and $\approx$30 mm (deposition probe), respectively, is calculated.

3.3. Source of impurities

There is a surprisingly large number of impurity species collected at the midplane probe. Besides deuterium and tungsten, Fe, Ni, Cr and Mn as components of the used stainless steel components (SS 301) can be detected and agree well with the elemental composition that is described for instance in [10]. 301 stainless steel consists of a Fe:Ni:Cr:Mn mixture of 75:6.6:17:0.8, whereas Fig. 4 (again measured at the sample during the flat-top phase at $t = 5$ s of #20823) reveals a ratio of 80:5:13:2. The origins of these impurities are stainless steel components not shielded from plasma view, mainly at the outer main chamber wall and additionally the outer covering of electric cables. These cables are moving slightly during discharges, resulting in development of cracks. Release of material by the cracks may lead to the formation of dust [11,12] which migrates through the machine and is subsequently redeposited at various positions – also at the midplane manipulator probe. Significant amounts of Ca and Mo as well as traces of Cl, P, Si, K, Al, F, Na, Mg, Ti, V and Cu are collected. Analysis of the isolation of electrical cables (between the actual conductor and the outer covering) used in ASDEX Upgrade reveals that their elemental composition mainly consists of Ca:K:Si:Ti at a ratio of 70:20:7:3 compared to a ratio of 84:6:6:4 found at the plasma edge. This fairly good agreement clarifies the origin of the most prominent impurities as a necessary condition for their reduction. An open question is still to what extent direct erosion fluxes from the IRCH antennas contribute to the amount of W found at the sample. The small radial decay length of W indicates, however, that transport through the scrape-off layer is the dominating process.

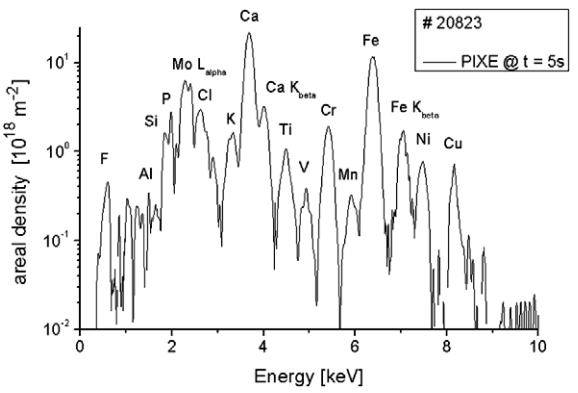

Fig. 4. PIXE spectrum corresponding to the flat-top phase of #20823. The lines are K_α emission if not otherwise indicated. The most prominent impurity Ca originates from the isolation material of cables. The stainless steel components Fe, Ni, Cr and Mn are detected at a ratio of 80:5:13:2 which resembles the elemental composition of 301 stainless steel.

4. Summary and outlook

Time resolved measurements of deuterium and impurity deposition on the midplane manipulator probe of ASDEX Upgrade are described. With decreasing distance to the separatrix the fluxes increase. Data are in good agreement with spectroscopic observations. Radial decay lengths in the limiter shadow are determined for start-up, flat-top and ramp-down phase of the plasma discharge. The origins of all observed impurity elements have been identified as first wall materials, stainless steel components and the isolation of electrical cables.

As next step laser ablation of W and comparison of midplane probe data with deposition at divertor probes will be performed and are expected to yield information about divertor retention and associated transport mechanisms. Variations in the radial decay length would result in different electron and ion temperatures and could therefore indicate different transport mechanisms, i.e. through the core or the edge plasma. Also the exposure of Si-targets is planned to measure the deposition flux of carbon and compare the results with those of the 2007 campaign with a complete W machine. A fast stroke into the outer core plasma will give information about the origin of collected impurities since it seems possible, that a fraction of the detected impurities originates from the core and that another fraction (especially W) is eroded at the ICRH limiters and transported in the edge plasma.

Acknowledgement

We acknowledge the help of R. Dux with the analysis of spectroscopic data and K. Schmid for providing TRIDYN calculations.

References

[1] G. JaneschitzITER, JCT and HTs, J. Nucl. Mater. 290–293 (2001) 1.
[2] R. Neu, J. Nucl. Mater., these Proceedings, doi:10.1016/j.jnucmat.2006.12.021.
[3] N. Peacock et al., in: P. Stott, G. Gorini, E. Sindoni (Eds.), Diagnostics for Experiment Thermonuclear Fusion Reactors, Varenna, Plenum, New York, 1996, p. 291.
[4] H. Maier et al., J. Nucl. Mater. 335 (2004) 515.
[5] K. Krieger et al., J. Nucl. Mater. 337–339 (2005) 10.
[6] M. Mayer, SIMNRA User's Guide, Report IPP 9/113, Max-Planck-Institut für Plasmaphysik, Garching, Germany, 1997.
[7] H. Paul, J. Sacher, Atom Data Nucl. Data Tables 42 (1989) 105.
[8] R. Dux, J. Nucl. Mater., these Proceedings, doi:10.1016/j.jnucmat.2007.01.014.
[9] J. Neuhauser et al., Plasma Phys. Control. Fusion 44 (2002) 855.
[10] T. Hong, M. Nagumo, Corros. Sci. 39 (9) (1997) 1665.
[11] J.P. Sharpe et al., Fusion Eng. Des. 63&64 (2002) 153.
[12] J. Winter, G. Gebauer, J. Nucl. Mater. 266–269 (1999) 228.